off to base-independent values at higher [OR^-], exactly as seen in Figure 9. The double reciprocal plot $(k_{obsd})^{-1}$ vs. $[OR^-]^{-1}$ should be linear and have the intercept $K_1/(k_eK_2K_bR_a)$ and an intercept/slope ratio equal to K_1. The K_1 value obtained in this manner from the 5.5 °C data of Figure 9 is 500 M^{-1}, within experimental uncertainty of the k_f/k_r ratio measured for adduct formation. The limiting k_{obsd} at high [OR^-] equals (intercept)$^{-1}$, i.e., $k_eK_2K_bR_a/K_1$, in this case 0.167 s^{-1}. The theoretical curve of Figure 9 was calculated with these values. At 25 °C similar interpretation of experimental results gave K_1 = 200 M^{-1} and k_{obsd}(lim) = 0.15 s^{-1}. If one makes the assumption that K_b is about the same as in aqueous methanol (0.13 at 25 °C) and that R_a is equal to the molality ratio $(m(H_2O)/m(CH_3OH) = 0.1)$ then $k_eK_2/K_1 \cong 15$ in the 50/48/2 THF/CH_3OH/H_2O mixed solvent. Given further the indications that $K_2/K_1 < 1$ (see above), one can estimate that k_e is substantially greater than 1 s^{-1} in this solvent. By comparison in 90/10 THF/H_2O k_{obsd}(lim) (2.e., k_e under these conditions) for the formation of $HFe(CO)_4^-$ was measured to be 0.1 s^{-1} at 25 °C. Thus it appears that k_e is larger in the more protic solvent, an observation suggesting that water or methanol may somehow mediate the transfer of hydrogen from the hydroxycarbonyl oxygen to the metal. A similar observation has been made by Catellani and Halpern, who noted that the platinum hydroxycarbonyl complex *trans*-[PtCl(CO_2H)(PEt_3)2] underwent decarboxylation more rapidly in the presence of water than in dry, aprotic solvents.[27,31a]

Summary

The present article has extensively examined the kinetics of the reactions of the oxygen nucleophiles CH_3O^- and OH^- with the pentacarbonyl compounds $M(CO)_5$ to give the methoxy- and hydroxycarbonyl adducts. Relative to the reaction with free CO[32], those with coordinated CO are dramatically activated. The heavier metal pentacarbonyls are the more reactive, but replacement of one CO by PPh_3 led to a substantial deactivation of the remaining carbonyls toward adduct formation. Methoxide proved to be a more powerful nucleophile than hydroxide under comparable conditions and both nucleophiles were more reactive in less polar solvent mixtures despite probable ion pairing with the counterions. The methoxycarbonyl adducts were stable but hydroxycarbonyl analogs underwent decarboxylation to give the respective metal hydride anions $HM(CO)_4^-$. In aqueous THF or the THF/CH_3OH/H_2O mixed solvent, decarboxylation occurs by a base and P_{CO} independent pathway proposed to be a "unimolecular" β-elimination.[33] This step did appear to be sensitive to the nature of the solvent and occurred at a faster rate in solvent systems containing a larger concentration of protic species. Our data also suggest that the base dependence of the WGSR catalysis by iron carbonyl, as described by King et al[34], is the result of the small values of K_2 (eq 20) combined with the low pH under catalysis conditions.

Acknowledgment. This work was supported by a contract with the U.S. Department of Energy, Office of Basic Energy Sciences. The ruthenium used in these studies was provided on loan by Johnson-Matthey Inc.

(31) In this context, Squires and co-workers have recently found that in the gas phase a $Fe(CO)_5/OH^-$ adduct believed to be the hydroxycarbonyl complex is quite stable and does not readily undergo decarboxylation. (Lane, K. R.; Lee, R. E.; Sallans, L.; Squires, R. R., submitted for publication. Private communication from R. R. Squires.)

(32) Free CO reacts slowly with aqueous base at elevated temperatures (Iwata, M. *Chem. Abstr.* **1969**, *70*, 6989r).

(33) A referee has suggested that rate-limiting CO dissociation from $Fe(CO)_4(CO_2H)^-$ prior to decarboxylation would be consistent with the P_{CO} independence of this reaction. If this step were irreversible, the kinetics would indeed be indistinguishable from those expected for direct decarboxylation of $Fe(CO)_4(CO_2H)^-$.

(34) King, A. D.; King, R. B.; Yang, D. B. *J. Am. Chem. Soc.* **1980**, *102*, 1028.

High-Resolution Solid-State ^{27}Al and ^{29}Si Nuclear Magnetic Resonance Study of Pillared Clays

D. Plee,[†] F. Borg,[‡] L. Gatineau,[†] and J. J. Fripiat*[†]

Contribution from CRSOCI, CNRS, 45045 Orleans Cedex, France, and the Laboratoire de Recherches, CFR, Harfleur, France. *Received July 9, 1984*

Abstract: This paper aims to define the short-range order structure in smectites pillared with aluminum polyhydroxy polymers so as to produce acid catalysts or catalyst supports with specific surface areas on the order of 300 m^2/g and pore sizes on the order of 8 × 10 × 10 $Å^3$. For that purpose the ^{27}Al and ^{29}Si nuclear magnetic resonance spectra of pillared smectites without substitution in the tetrahedral layer (hectorite and laponite) or with substitutions in the tetrahedral layer (synthetic beidellite) have been recorded under the condition of magic angle spinning. In uncalcined samples, the main conclusion of this study is that the pillaring agent is the so-called Al_{13} polymer made from 12 Al octahedra surrounding 1 Al tetrahedron. When pillared smectites without tetrahedral substitution are calcined, there is no reaction between pillars and the smectite surface. On the contrary, in pillared beidellite a deep structural transformation occurs that can be interpreted as the growth of a tridimensional network grafted on the bidimensional network of the clay. The resulting high-area solid could be considered as a "bidimensional zeolite". Its acidic properties are indeed comparable with those of Y zeolites and much stronger than those of calcined pillared smectites without tetrahedral substitution.

The main purpose for pillaring a swelling clay is to keep a large fraction of the internal surface area available for adsorption and eventually for catalytic processes. Indeed smectites like dioctahedral montmorillonite or trioctahedral hectorite swell upon adsorbing polar reagents, but they lose their expanding properties after a heat treatment in a temperature range where adsorbent regeneration or catalytic reactions are carried out. The total surface areas (external plus internal) of swelling clays are close to the theoretical limit for a bidimensional sheet silicate, namely 800 m^2/g. The external surface area is usually lower than ~80 m^2/g. Since montmorillonite has been pillared with aluminum

[†] CRSOCI, CNRS.
[‡] Laboratoire de Recherches, CFR.

0002-7863/85/1507-2362$01.50/0

hydroxy polymers, it is now well established that clays with specific surface areas of about 250 m^2/g and d_{00l} spacings of about 18 Å can be synthesized and that these characteristic parameters are maintained more or less constant after heating to about 500 °C (see, for instance, ref 1–5).

Such pillared clays can be obtained from different procedures. For instance, Lahav et al.[1,2] have used aluminum hydroxy polymers prepared from Al^{3+} solutions, the pH of which was adjusted such that the OH/Al ratio was on the order of or smaller than 2.3. These positively charged polymers are cation exchanged with the negatively charged clay, and the resultant solid is washed to remove the excess aluminum species. Vaughan et al.[3] have used the so-called aluminum chlorhydrol solution, which is hydrolyzed in the clay slurry. Jacobs et al.[6] have achieved pillaring by dialyzing relatively concentrated clay–aluminum hydroxy polymer slurries. It is rather surprising that from all these procedures pillared clays with quite similar surface areas and d_{00l} spacings are obtained whereas earlier works, for instance, by Hsu[7] and Poncelet and Brindley,[8] lead to the formation of what can be considered aluminum chlorites. In those works one layer of aluminum hydroxide was intercalated within the clay interlamellar space and d_{00l} was about 14.5 Å. The main difference between the procedures leading either to large expansion (~18 Å) or to small expansion (~14 Å) must first find its origin in a different structure of the intercalated species. Indeed since the basal distance of a thoroughly dehydrated smectite is of the order of 10 Å, the aluminum hydroxide species leading to the 14-Å complex may have the structure of an elementary aluminum trihydroxide sheet composed of two layers of hydroxyls with octahedral sites only. The 18-Å expansion requires the presence of bulkier alumina species with perhaps four oxygen or hydroxyl layers. Also, in view of the large increase of the surface area and the thermal stability of the 18-Å pillared clay, the aluminum hydroxy polymers leading to that complex must have a rather limited "lateral" expansion since they fill only partially the interlamellar space providing a large internal surface area. Typically the 14-Å pillared clays are obtained either by cation exchanging the clay with Al^{3+} and increasing the pH above 5 or by mixing an aluminum hydroxide slurry with a clay suspension.

The nature of polymeric aluminum hydroxide species in solution is still debated. Brosset et al.[9] using potentiometric techniques suggested the formation of oligomers like $[Al_6(OH)_{15}]^{3+}$ or $[Al_8(OH)_{20}]^{4+}$ whereas Hsu and Bates[10] advocated the growth of polymers made from the basic unit $[Al_6(OH)_{12}(H_2O)_{12}]^{6+}$ at increasing pHs.

Using small-angle X-ray scattering, Rausch and Bale[11] suggested that for OH/Al ratios between 1.5 and 2.5, a polymer $[Al_{13}O_4(OH)_{24}(H_2O)_{12}]^{7+}$ composed from 12 Al octahedra and 1 Al tetrahedron exists in solution. This cationic species had been previously studied in the crystalline state by Johansson.[12] A "blown up" representation of this polymer, hereafter referred to as Al_{13}, is shown in Figure 1. Indeed Akitt et al.[13] and Bottero et al.[14] were able to identify by ^{27}Al NMR a species giving a signal shifted by about δ +61 with respect to $[Al(H_2O)_6]^{3+}$ taken as reference. This signal was assigned to tetrahedral Al in Al_{13}. The signal due to octahedral Al in this complex gave such a broad line that it could not be observed at the same expansion scale as the tetrahedral species. The obvious explanation is that the lack of symmetry of the octahedron increases strongly the quadrupole coupling constant whereas the symmetry of the tetrahedral site in the structure shown in Figure 1 is not so distorted. The Al_{13} concentration seems to be mostly dependent on the OH/Al ratio. The total concentration in Al between 0.06 and 0.5 M has much less influence.[15] The other aluminum species suggested by Bottero et al.[14] are either monomeric $[Al(OH)_x(H_2O)_{6-x}]^{(3-x)+}$ or dimeric $[Al_2(OH)_x(H_2O)_{10-x}]^{(6-x)+}$.

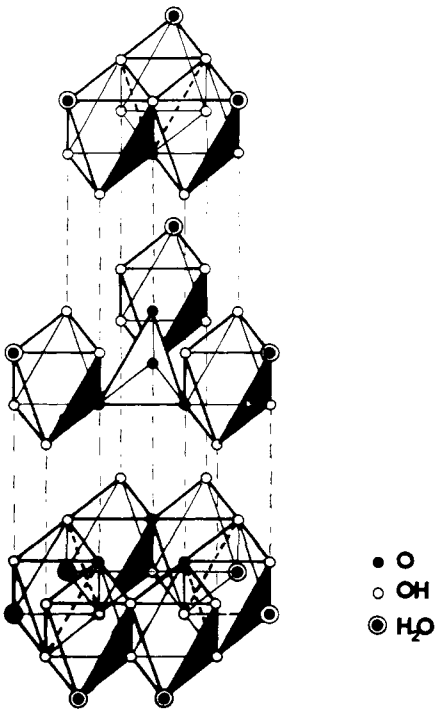

Figure 1. Blown up atomic model of the $Al_{13}O_4(OH)_{24}^{7+}$ polymer.

According to Van Cauwelaert et al.,[16] considering solutions in which OH/Al < 2.3 as composed from three components is perhaps an oversimplification. There might be a distribution of polymers with various Al^{IV}/Al^{VI} ratios (the roman numerals IV and VI stand for the coordination with respect to oxygen).

The Al_{13} polymer shown in Figure 1 contains the four layers of superimposed oxygen atoms (or water or hydroxyls) that would be needed to expand the clay basal spacing to 18 Å. That this species is responsible for the 18-Å pillared clays has been suggested by Vaughan et al.[3] Another argument also in favor of this hypothesis is the limited lateral expansion of this polymer. The surface area occupied by one polymeric unit is about 110 $Å^2$, as measured from an atomic model.

So far, however, the experimental evidences for assuming that pillaring at 18 Å is due to the intercalation of Al_{13} are indirect, and in addition, nothing is known either about the thermal transformation of the pillars or about the link between pillars and clay sheets before and after thermal treatment.

In order to investigate this point, the behaviors of clays with negative charges smeared out on the lattice or with localized negative charges need to be studied. Montmorillonite and hectorite are good examples of the former case whereas beidellite is an example of the latter. Thus in this study, pillared hectorite and synthetic beidellite will be compared. Only techniques able to give information on short-range atomic organizations can detect the actual nature of the pillars or the link between pillars and sheets since X-ray diffraction data show that the long-range order

(1) Lahav, N.; Shani, U.; Shabtai, J. *Clays Clay Miner.* **1978**, *26*, 107.
(2) Lahav, N.; Shani, U. *Clays Clay Miner* **1978**, *26*, 116.
(3) Vauchan, D. E. W.; Lussier, R. J. "Proceedings of the International Conference on Zeolites, 5th"; Rees, L. V., Ed.; Heyden: London, 1980; p 94.
(4) Pinnavaia, T. J. *Science (Washington, D.C.)* 1983, *220*, 365.
(5) Brindley, G. W.; Sempels, R. E. *Clay Miner.* **1977**, *12*, 229.
(6) Jacobs, P.; Poncelet, G.; Schutz, A. Fr. Pat. 2512043, 1982.
(7) Hsu, P. H. *Clays Clay Miner.* **1968**, *16*, 303.
(8) Poncelet, G.; Brindley, G. W. *Am. Mineral.* **1967**, *52*, 1161.
(9) Brosset, C.; Biedermann, G.; Sillen, L. G. *Acta Chem. Scand.* **1954**, *8*, 1917–1926.
(10) Mesmer, R. E.; Baes, C. F. *Inorg. Chem.* **1971**, *10*, 2290.
(11) Rausch, W.; Bale, H. D. *J. Chem. Phys.* **1964**, *40*, 3891.
(12) Johansson, G. *Acta Chem. Scand.* **1960**, *14*, 771.
(13) Akitt, J. W.; Greenwood, N. N.; Khandelval, B. L.; Lester, G. R. *J. Chem. Soc., Dalton Trans.* **1972**, 604.
(14) Bottero, J. Y.; Cases, J. M.; Fiessinger, F.; Poirier, J. E. *J. Phys. Chem.* **1980**, *84*, 2933.
(15) Bottero, J. Y.; Marchal, J. P.; Poirier, J. E.; Cases, J. M.; Fiessinger, F. *Bull. Soc. Chim. Fr.* **1982**, 439.
(16) Van Cauwelaert, F. H.; Bosmans, H. *Rev. Chim. Miner.* **1969**, *6*, 611.
(17) Bottero, J. Y.; Tchoubar, D.; Cases, J. M.; Fiessinger, F. *J. Phys. Chem.* **1982**, *86*, 3667.

Table I. Total Water Content (Hydration + Constitutional) (%) of Samples Submitted to MAS-NMR

B	11.5	PH	26.1	PL	22.3
PB	45	CPH	15.3	CPL	16
CPB	11.6				

is rather poor. Indeed at best only the first six 00*l* reflections are observed on an oriented aggregate whereas *hk*0 reflections are very broad and weak.

It is for these reasons that this high-resolution solid-state magic angle spinning nuclear magnetic resonance (MAS-NMR) study of the ^{27}Al and ^{29}Si nuclei has been undertaken. In the few years since the pioneering works of Lippmaa et al.,[18,19] MAS-NMR has become a powerful tool for studying aluminosilicates as shown by a rapidly increasing number of papers (ref 20–23, for instance, and references therein). However, as far as we are aware, it has not been applied to pillared clays.

Experimental Section

Materials. The smaller than 2-μm fraction of hectorite (Hector, CA) was used after elimination of carbonates in order to prepare the pillared hectorite (PH) according to the procedure described by Jacobs et al.[6] A synthetic magnesium silicate, laponite (Laporte Ind., U.K.), was used as such and pillared in the same way (PL). None of these minerals contained detectable amounts of Al (by NMR) before pillaring. After they were pillared and before calcination, both gave a d_{00l} spacing of ~18.5 Å, which reduces to 18–17.5 Å after calcination at 300–400 °C. The calcined samples are denominated CPH and CPL. Synthetic beidellite (B) and pillared beidellite (PB) were obtained according to the procedure described by Fripiat and Plee[24].

On the basis of the solids calcined at 900 °C such that all constitutional and hydration water molecules are not taken into consideration, the structural formulas calculated from the chemical analysis performed on the hydrated solids are as follows (average of five different samples): B, $Na_{0.9}(Si_{7.1}Al_{0.9})^{IV}Al_4^{VI}O_{22}$; PB, $Na_{0.06}1.51Al^{(13)}(Si_{7.1}Al_{0.9})^{IV}Al_4^{VI}O_{23.8}$, where, $Al^{(13)}$ represents one aluminum atom in one hydroxy polymer unit (Figure 1). CPB was obtained after heating PB at 400 °C for 3 h. The spacings in PB and CPB were quite comparable with those of PH or of any montmorillonite pillared at 18 Å, but the surface area, the porosity, the molecular sieving, and catalytic properties of CPB are different from those of a calcined pillared montmorillonite, as shown elsewhere.[24,25] The total water contents of the materials in their hydratation state when the MAS-NMR spectra were recorded are indicated in Table I.

Bayerite, $Al_2(OH)_6$, and the transition η-alumina obtained by dehydroxylating bayerite were used as references for ^{27}Al MAS-NMR.

Instruments. The ^{29}Si and ^{27}Al spectra were recorded by using two spectrometers operating at 8.45 and 11.7 T, respectively, and equipped with Nicolet 1180 and 1280 computers for data acquisition. The Fourier transform kits were those described by Meadows et al.,[26] and the spectra were recorded at the facilities of the Department of Chemistry at the University of Illinois (Urbana-Champaign). The magic angle sample-spinning assemblies were those of Andrews.[27] The rotor used for ^{29}Si contained about 200 mg of material whereas that used for ^{27}Al could accommodate about 75 mg. Chemical shifts are reported in ppm relative to 1 M $[Al(H_2O)_6]^{3+}$ for ^{27}Al and to tetramethylsilane (Me_4Si) for ^{29}Si. All samples studied were low enough in paramagnetic impurities to keep the full width at half-height (fwhh) on the order of 5 ppm for ^{29}Si and 5–25 ppm for ^{27}Al.

Table II. Chemical Shifts of the ^{29}Si MAS-NMR Line According to the Number of Fourfold Coordinated Aluminum Nearest Neighbors (Si-*n* Al, $O \le n \le 4$)[a]

Si environment	Si–0 Al	Si–1 Al	Si–2 Al	Si–3 Al	Si–4 Al
phyllosilicate	99–93	90–85	86–84	~76	*b*
zeolite	114–102	107–96	102–93	97–88	89–80

[a] Data from Fyfe et al.[20] for zeolites and from Kinsey et al.[21] for phyllosilicates (−δ, ppm with respect to Me_4Si). [b] Unknown.

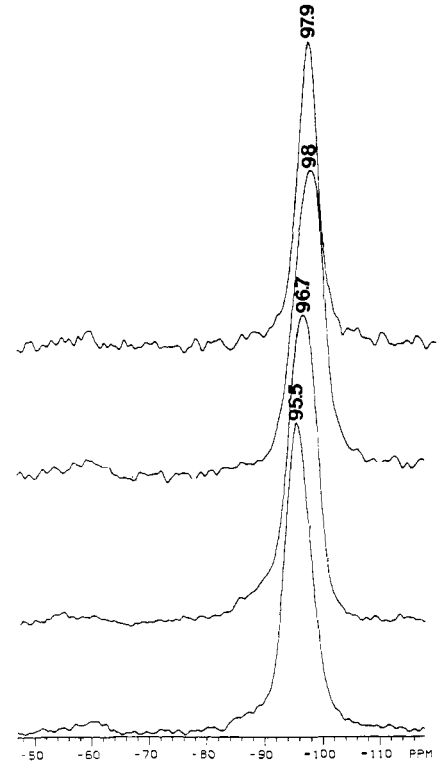

Figure 2. 8.45-T ^{29}Si MAS spectra, corresponding to a resonance frequency of 71.52 MHz, of pillared hectorite and laponite. Experimental conditions: 800 scans at 10-s recycle time; 12-μs 90° pulse; 20-μs delay before acquisition; 8192 data points on ±25 kHz; 50-Hz line broadening. From top: Si_4, 2.7-kHz MAS spectrum of pillared hectorite (PH); Si_5, 2.7-kHz MAS spectrum of calcined pillared hectorite (CPH); Si_7, 2.6-kHz MAS spectrum of calcined pillared laponite (CPL); Si_6, 2.5-kHz MAS spectrum of pillared laponite (PL).

Results

Quantitative determinations. The ^{27}Al and ^{29}Si spectra can be decomposed into various contributions corresponding to different shieldings and thus to different atomic environments.

^{29}Si NMR Spectra. For the ^{29}Si nucleus (spin $I = {}^1/_2$) the chemical shift is affected mainly by the electronic density on the oxygen atoms of the silicon tetrahedron. Therefore the nature of the neighboring atoms, linked or coordinated to these oxygen atoms, may be expected to influence the shift. The more positive the chemical shift is, the weaker the shielding.

Table II shows the approximate ranges of δ reported for the tridimensional silicate framework of zeolites and for the bidimensional framework of sheet silicates.

The spread of those shifts is not only a function of the structural disorder but it depends also on the nature of the second neighbors.[23] This may be the reason why for the same next nearest neighbors there are significant differences between phyllosilicates (or sheet silicates) and tectosilicates. In order to obtain the relative contributions of each type of environment, the complex ^{29}Si signal was decomposed into its components. This was carried out (i) by assuming a Gaussian shape for each component and (ii) by varying their fwhh and the position of the maximum so as to obtain the best fit between the observed and simulated signal. It was verified that introducing slightly asymmetrical components was not necessary for obtaining the smallest error, as shown further.

(18) Lippmaa, E.; Magi, M.; Samoson, A.; Engelhardt, G.; Grimmer, A. R. *J. Am. Chem. Soc.* **1980**, *102*, 4889.
(19) Lippmaa, E.; Magi, M.; Samoson, A.; Tarmak, M.; Engelhardt, G. *J. Am. Chem. Soc.* **1981**, *103*, 4992.
(20) Fyfe, C. A.; Thomas, J. M.; Klinowski, J.; Gobbi, G. C. *Angew. Chem., Int. Ed. Engl.* **1983**, *22*, 259.
(21) Kinsey, R. E.; Kirkpatrick, R. J.; Hower, J.; Smith, K. A.; Oldfield, E., submitted for publication in *Am. Mineral.*
(22) Kirkpatrick, R. J.; Kinsey, R. E.; Smith, K. A.; Henderson, D. M.; Oldfield, E., submitted for publication in *Am. Mineral.*
(23) Sanz, J.; Serratosa, J. M. *J. Am. Chem. Soc.* **1984**, *106*, 4790.
(24) Plee, D.; Fripiat, J. J.; submitted for publication in *Clays Clay Miner.*
(25) Plee, D.; Shutz, A.; Poncelet, G.; Fripiat, J. J., paper presented in part at the International Symposium on Catalysis by Acids and Bases, Villeurbanne, France, 1984; submitted for publication in *Surf. Sci.*
(26) Meadows, M. D.; Smith, K. A.; Kinsey, R. E.; Rothgeb, T. M.; Skarjune, R. C.; Oldfield, E. *Proc. Natl. Acad. Sci. U.S.A.* **1982**, *79*, 1351.
(27) Andrews, E. R. *Prog. Nucl. Magn. Reson. Spectrosc.* **1973**, *8*, 1.

Table III. ^{29}Si Chemical Shifts ($-\delta$, ppm), fwhh (ppm), and Relative Contributions (%) of Si–*n* Al Components Obtained Using the Decomposition into Three Gaussians[a]

		Si–0 Al		Si–1 Al		Si–2 Al		
spectrum	fwhh, ppm	%	δ	%	δ	%	δ	sample
1	4.9	66.7	95.5 (95.2)	30	90.3 (90.2)	3.3	85.6	B
2	3.5	63.4	95.6 (95.9)	31.2	90.8 (91.2)	5.4	87	PB
3	5.5	65.8	96.8 (96.2)	28.2	92.4	6	86.5	CPB
4	4.1	100	97.9					PH
5	6.1	100	98					CPH
6	5.2	100	95.5					PL
7	5.9	100	96.7					CPL

[a] The position of the observed peak maxima is in parentheses.

Table IV. $(Al/Si)^{IV}_s$ Ratio Obtained with Eq 1 and Theoretical Relative Intensities of Si–*n* Al Components in the ^{29}Si Spectra Obtained for a Random Distribution of Al Obeying the Loewenstein Rule[a]

	$(Al/Si)^{IV}_s$, %		Si–0 Al, %		Si–1 Al, %		Si–2 Al, %		fwhh,
sample	ch	exptl	theor	exptl	theor	exptl	theor	exptl	ppm
B	0.127	0.122	63	66.7	32	30	5	3.3	4.9
PB	0.127	0.140	63	63.4	32	31.2	5	5.4	3.5
CPB	0.127	0.134	63	65.8	32	28.2	5	6	5.5

[a] Reference 28. The experimental values are those of Table III.

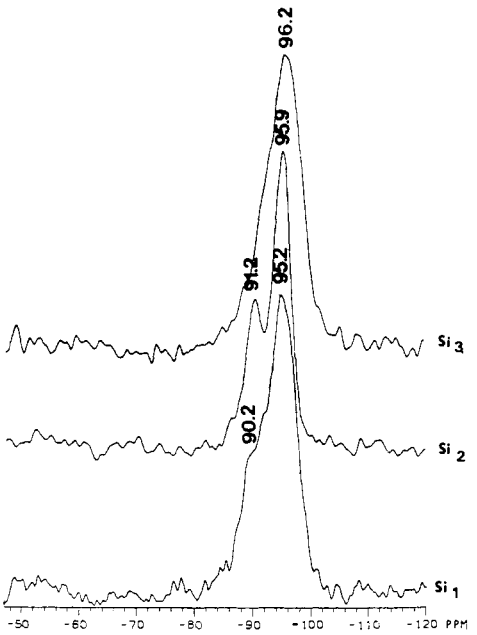

Figure 3. 8.45-T ^{29}Si spectra, corresponding to a resonance frequency of 71.52 MHz, of CPB (Si_3), PB (Si_2), and beidellite (B; Si_1). MAS frequency: 2.7 kHz for Si_1, 2.5 kHz for Si_2, and 2.6 kHz for Si_2. Other experimental conditions as in Figure 2.

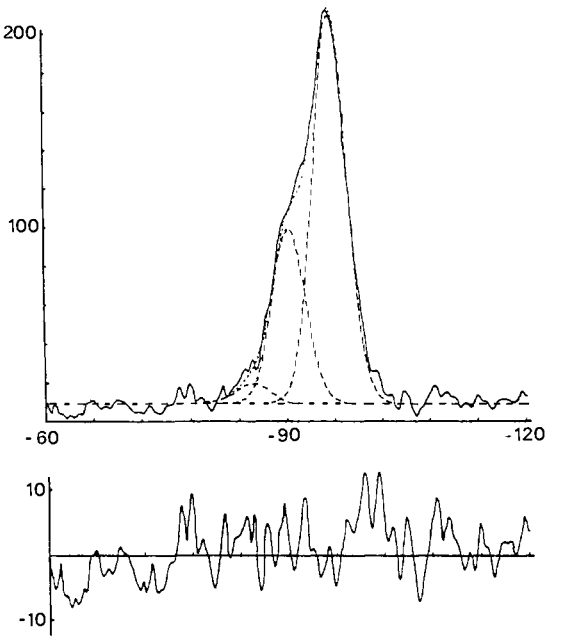

Figure 4. Top: decomposition of the ^{29}Si MAS spectrum of B (Si_1), shown in Figure 3, into three Gaussian contributions with fwhh = 4.9 ppm. The experimental spectrum is the full time. The dotted line is the simulation spetrum. The three components are represented with dashed lines. Bottom: residuals.

Using Lorentzian-shaped peaks did not lead to any significant improvement.

Figure 2 shows the ^{29}Si spectra obtained for PH, CPH, PL, and CPL, namely for uncalcined and calcined pillared clays that do not contain structural aluminum. In those clays, the aluminum cations are only in the pillars. It is obvious that in those samples there is a single ^{29}Si line width fwhh (see Table III) between 4 and 6 ppm and δ between 96 and 98 ppm. Calcination increases slightly the width of the line.

By contrast the ^{29}Si lines observed for B, PB, and CPB shown in Figure 3 contain at least two and perhaps three components with less negative shift. By use of the deconvolution procedure briefly described in the Experimental Section, acceptable simulation spectra were obtained with three Gaussian components, as shown by an example in Figure 4. The fwhh and the peak maxima are those shown in Table III. For the B and PB spectra the residuals were of the same order of magnitude. Decomposition in two Gaussian components leads to higher residuals.

The chemical shift values used for fitting the observed ^{29}Si spectra are in rather good agreement with those reported in Table II for phyllosilicates in which silicon tetrahedrons have zero, or two aluminum tetrahedrons as first neighbors.

For further discussion it is worth mentioning that the Si–1 Al component in CPB is slightly more negative shifted (δ -92.4) than in PB and B. Thus in CPB the component is shifted toward the range reported for tridimensional zeolites.

The actual significance of the deconvolution procedure used for obtaining the relative intensities of the three contributions to the ^{29}Si spectra shown in Table II can be checked in two ways.

First, the random distribution of silicon and aluminum sites on a network representing the tetrahedral layer can be simulated on a computer by using as a variable the relative $(Al/Si)^{IV}$ content and compelling the system to obey the Loewenstein rule,[28] which states that two aluminum tetrahedrons cannot be nearest neighbors. The agreement between the theoretical (theor) values obtained from that simulation and those obtained from the ^{29}Si

(28) Loewenstein, W. *Am. Mineral.* **1954**, *39*, 92.

Table V. ^{27}Al Chemical Shifts (δ, ppm), fwhh (ppm), and Relative Contributions of Tetrahedrally and Octahedrally Coordinated Species

	Al^{IV}_s			$Al^{IV}_{p(or\ z)}$			Al^{VI}				
no.	%	δ	fwhh	%	δ	fwhh	%	%	δ	fwhh	sample
1	24	69.3	7				24	76	3	9.2	B
2	22	69.1	5.7	6	62.3	2.2	28	72	3.4	8.8	PB
3	10	67.5	11.4	(4.5)	(56.5)	14	14.5	85.5	2.6	8.7	CPB
4				10	61	26.2	10	90	6.8	15.8	PH
5				18.5	59.1	18.4	18.5	81.5	5.9	14	CPH
6				21	59.3	26.3	21	79	7.1	11.1	PL
7				37	63.5	24.5	37	63	4.8	15.7	CPL
8							0	100	8	16.6	bayerite
9	30	68.1	19.3				30	70	8.9	16.2	η-Al_2O_3

spectra decomposition (exptl) is satisfactory, as shown in Table IV. In addition, these calculations have shown that the eventual Si-3 Al or Si-4 Al components would contribute less than 1%.

Second, it is possible to predict the ratio $(Al/Si)^{IV}$ in the tetrahedral layer from the relative experimental contributions of each I(Si-n Al) component by using the relationship

$$(Al/Si)^{IV} = \sum_0^n \frac{n}{3} I(\text{Si-}n\ \text{Al}) \qquad (1)$$

Here also the agreement between the ratios obtained either in that way (exptl) or from the chemical formulas (ch) is quite good (Table IV, first column).

^{27}Al NMR Spectra. For ^{27}Al, which has spin $I = {}^5/_2$, the $m = {}^1/_2$, $m = -{}^1/_2$ transition is independent of quadrupolar interaction of first order but is affected by second-order quadrupolar effects. Large variations of the quadrupole coupling constant provoke distortion of the peak shape because of the increasing influence of second-order terms. The sideband patterrn is also modified. The quadrupole coupling constant being the product of the quadrupole moment by the electrical field gradient at the nucleus, the peak shape is very sensitive to change in the symmetry of the coordination shell and in the distribution of electrical charges. Here also in first approximation, the weaker the shielding, the more positive the shift.

The highest available field, namely 11.7 T, was used for ^{27}Al in order to decrease as much as possible the effect on the shift of the second-order quadrupolar effect.[22] In all ^{27}Al spectra observed in this work, tetrahedral and octahedral ^{27}Al can be separated and the data acquisition system carries out the integration of the relative intensity of the two lines and of their sidebands, allowing a semiquantitative determination of the two types of sites. An example of an ^{27}Al spectrum and of the integration procedure in shown in Figure 5 for η-Al_2O_3.

Bayerite shows only one central line with two sidebands, whereas in η-Al_2O_3 30% of the signal intensity is associated with the component observed at δ 68.1 and assigned to Al^{IV}. The Al^{VI} central line is at δ 8.9. From the electron radial distribution in Al_2O_3, Leonard et al.[29] have measured an Al^{IV} relative content of 33%, in agreement with the theoretical number of tetrahedral sites in a spinel structure. This example was shown in order to outline the degree of reliability of the quantitative determinations obtained for ^{27}Al in two different environments when the two peaks have about the same fwhh (see Table V).

For PH, CPH, PL, and CPL, the spectra are shown in Figure 6. The central line between 5 and 7 ppm can be assigned to Al^{VI} in the pillar (Al^{VI}_p). Two sidebands are clearly visible. The line between 59 and 63 ppm is most probably that of Al^{IV} in the Al_{13} polymer (Al^{IV}_p). The NMR spectrum of this species in aqueous solution contains that line at δ 61 ± 1 according to Bottero et al.[14] The ^{27}Al NMR spectrum of the hydroxylaluminum pillaring solution that has been used in this work is entirely similar to those shown in ref 14.

As far as we are aware, the spectra in Figure 6 present the first direct spectroscopic evidence supporting the hypothesis proposed by Vaughan et al.[3] and also by Pinnavaia[4] that the Al_{13} polymer is indeed the pillaring species. As recalled before, in solution, the

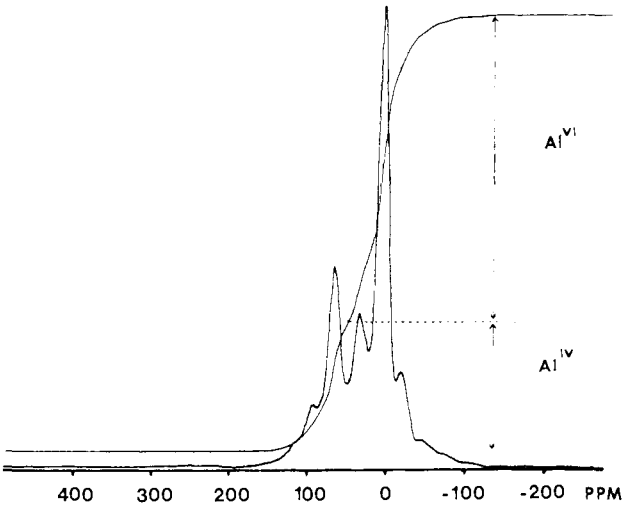

Figure 5. Example of the integration procedure applied to the η-Al_2O_3 spectrum.

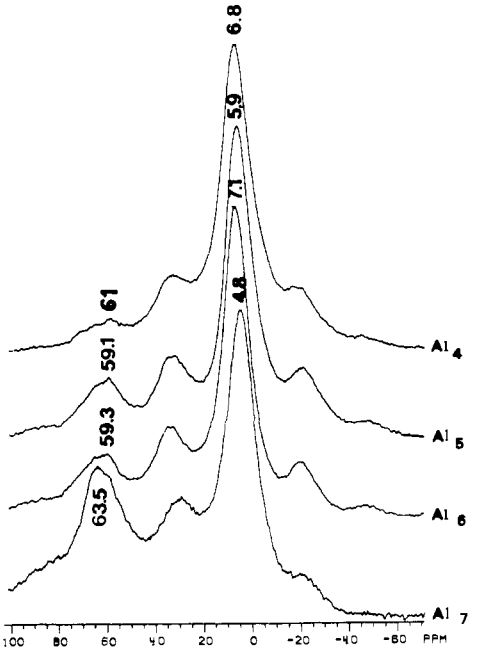

Figure 6. 11.7-T ^{27}Al MAS spectra, corresponding to a resonance frequency of 130.3 MHz, pillared hectorite (PH; Al_4), calcined pillared hectorite (CPH; Al_5), pillared laponite (PL; Al_6), and calcined pillared laponite (CPL; Al_7). Experimental conditions: 500 scans at 0.1-s recycle time; 4-μs 90° pulse; 10-μs delay before acquisition; 8192 data points on ±50 kHz; 50-kHz line broadening; 3.5-kHz MAS frequency.

Al^{VI} octahedra in Al_{13} are not observed. However, in the pillared hectorite and laponite and under the MAS conditions, the signal of Al^{VI}_p is the most intense, as shown in Table V.

The relative intensities of the lines assigned to Al^{IV}_p or Al^{VI}_p are not those expected on the basis of the structure of the Al_{13}

(29) Leonard, A. J. *Semaille*, P. N.; Fripiat, J. J. *Proc. Br. Ceram. Soc.* **1969**, 103.

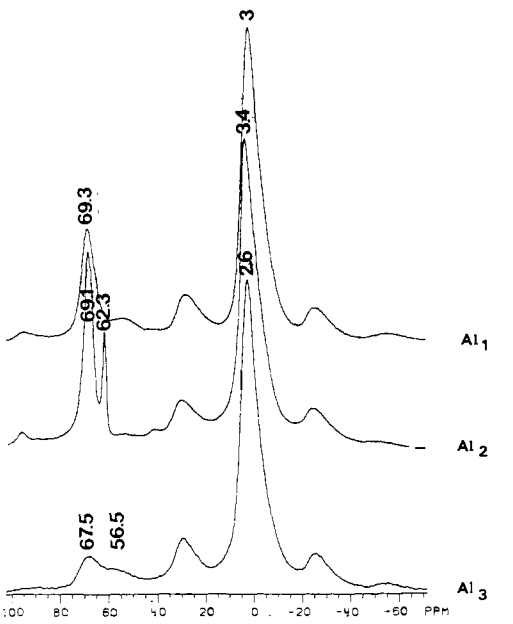

Figure 7. 11.7-T ^{27}Al MAS spectra, corresponding to a resonance frequency of 130.3 MHz, of beidellite (B; Al_1), pillared beidellite (PB; Al_2), and calcined pillared beidellite (CPB; Al_3). Experimental conditions as those given in Figure 6.

species which contains ideally about 8% Al^{IV}_p. This is near what is observed for PH. In CPH, however, the Al^{IV}_p relative content increases by almost a factor of 1.8. The same relative increase is observed in CPL as compared to PL. In PL the Al^{IV}_p relative content is already 21% in the uncalcined sample.

There is no obvious reason why the Al^{IV}_p content should be higher in the pillared clays than in the starting polymer and moreover no reason for that content to increase upon calcination. An explanation could be that a fraction only of Al^{VI}_p species is observed. Indeed if the octahedral sites are distorted, a fraction of the octahedral aluminum could escape detection.

If the pillar was transformed upon calcination into something similar to a transition alumina, the tetrahedral aluminum signal should appear at a higher shift (68.1 ppm in η-Al_2O_3).

The difficulty in interpreting quantitatively the ^{27}Al spectra is well-known. When the quadrupole coupling constant is very large, a complex sideband pattern for the central transition is observed (Ghose et al.[30]). Consider for instance the spectra of Figure 6. In PH (Al_4 spectrum) the central band due to Al^{VI}_P is strong and the two sidebands have about the same intensity whereas in CPL (spectrum Al_7) the sideband shifted negatively with respect to the central band is much weaker than that shifted positively.

The ^{27}Al spectra of B, PB, and CPB samples are shown in Figure 7. The spectrum of the synthetic beidellite has main lines at 3 and 69.3 ppm, which are assigned to octahedral (Al^{VI}_s) and tetrahedral (Al^{IV}_s) aluminum, respectively, in agreement with Kinsey et al.[21] Observe that the fwhh of these lines are noticeably narrower than those of Al^{IV}_p and Al^{VI}_p in PH and PL (Table V).

The relative contribution of Al^{IV}_s to the ^{27}Al spectrum (24%) is not too far from that calculated from the chemical formula, namely 18.5%. It is worth remembering that a structural chemical formula is valid under the assumption that the chemical analysis refers to a single phase. The presence of small amounts of amorphous materials in the hydrothermal beidellite, undetectable by X-ray diffraction, could lead to rather large errors in calculating Al^{IV}_s.

In PB, the most important feature is the observation of two kinds of tetrahedral sites at δ 69.1 and 62.3. the assignment of the former to Al^{IV}_s and of the latter to Al^{IV}_p seems obvious. Again, however, there exist quantitative disagreements between the distribution of aluminum upon the four potential types of sites, namely Al^{IV}_p, Al^{IV}_s, and $Al^{VI}_s + Al^{VI}_p = Al^{VI}$ shown in Table V, and the results of the chemical analyses according to which there should be 1.8% Al^{IV}_p, 14% Al^{IV}_s, and 84.2% ($Al^{VI}_s + Al^{VI}_p$). The very narrow fwhh of the line assigned to Al^{IV}_p in Al_{13} is probably due to the high hydration water content in PB (see Table I).

In spite of the difficulty of interpreting quantitatively the ^{27}Al spectra, a common and important conclusion appears for all the pillared clays in the sense that the pillaring species is the Al_{13} polymer.

Upon calcination of PB at 300 °C, the ^{27}Al spectrum is strongly modified. In spite of observing a reinforcement of the Al^{IV} signal as in CPH and CPL, not only the Al^{IV}_s signal decreases in intensity but also it tails toward lower shifts, a shoulder being observed around δ 56.5. No defined peak appears at the shift where Al^{IV}_p should be observed. It is worth pointing out that in feldspars the signal assigned to tetrahedral aluminum is observed with an average shift of 58 ± 3 ppm, as it results from 15 spectra reported by Kirkpatrick et al.[22]

The shoulder at 56.5 ppm could be related to the more negative shift observed for ^{29}Si in the Si-1 Al contribution in CPB, as compared to PB and B. Both observations suggest that calcination of PB induces a reaction between the Al polymer and the aluminum-substituted tetrahedral layer of the beidellite, resulting in stronger shielding of ^{29}Si in Si-1 Al and the ^{27}Al species Al^{IV}_z at δ 56.5. It is of course tempting to suggest that there is a link between these two observations.

Short-Range Ordering in Calcined Pillared Beidellite (CPB). The higher shielding of the silicon nucleus in some Si-1 Al linkages and the less positive shift of Al^{IV}_z suggest strongly that calcining the pillared beidellite provokes important structural rearrangements.

If one has to predict what kind of reaction may occur between Al_{13} polymers and the tetrahedral layer directly in contact, one has to find reactive sites in that layer. It is well-known that in a tetrahedral layer the weakest point is the aluminum tetrahedron. For instance, in ammonium beidellite removal of ammonia leads to the reaction schematized as follows:

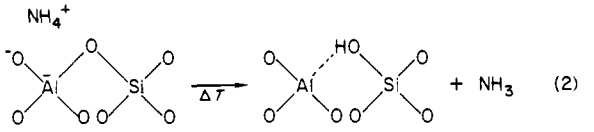

(2)

Indeed SiOH stretching bands at 3420 and 3500 cm^{-1} have been observed.[31] Such a reaction is very comparable to the decationation reaction described for the first time in X and Y zeolites by Uytterhoeven et al.[32]

The Al_{13} species being acidic, it may be expected that protons would be liberated upon calcination. These protons should open silicon–oxygen–aluminum bridges near aluminum sites of the tetrahedral layer, and the reaction of these acidic OH with pillar peripheral OH's, bonded to Al^{VI}_p, would anchor the pillars to the layer. This reaction would not occur with pillared hectorite and montmorillonite, which are ideally free from tetrahedral substitution.

The reaction between protonated Si–OH–Al^{IV}_s bridges and pillars yields either Si–O–Al^{VI}_p or Al^{IV}_s–O–Al^{VI}_p linkages. In the first case the nearby Al^{IV}_s may complete its coordination shell with a water molecule, whereas in the second case the formation of a silanol group is probable.

If the pillar-to-sheet linkage is of the first type, the intensity of the Si-1 Al contribution to the ^{29}Si resonance line should decrease whereas the frequency of that line would not shift appreciably because the nature of the cation in the second coordination shell would not change (Al^{VI}_s replaced by Al^{VI}_p). From Table III it is clear that the intensity of the Si-1 Al^{IV}_s contribution does not decrease, but the line shifts by about 2 ppm toward a more negative value.

(30) Ghose, S.; Tsang, T. *Am. Mineral.* **1973**, *58*, 748.

(31) Chourabi, B.; Fripiat, J. J. *Clays Clay Miner.* **1981**, *29*, 260.

(32) Uytterhoeven, J. B.; Christner, L. G.; Hall, W. K. *J. Phys. Chem.* **1965**, *69* 2117.

(33) Dubinin, M. M.; *J. Colloid Interface Sci.* **1967**, *23*, 489.

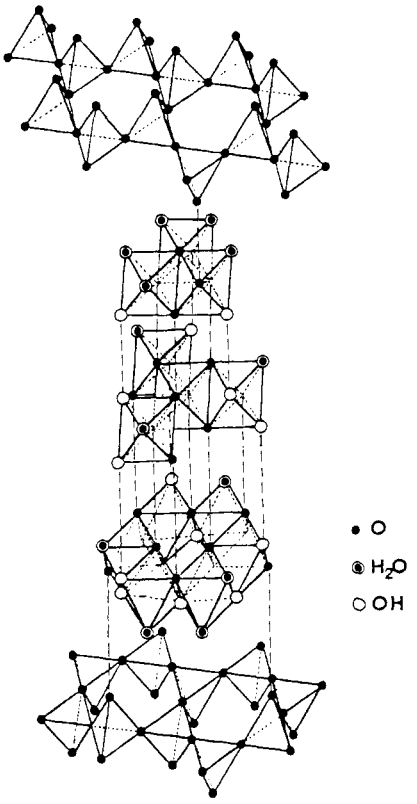

Figure 8. Schematic structure of CPB. "Blown up" structure of the thermally modified pillars sharing three oxygen atoms with three inverted Al^{IV}_z tetrahedra of two tetrahedral clay layers.

If anchoring the pillar to the sheet is obtained through the formation of Al^{IV}_s–O–Al^{VI}_p linkages, the intensity of the Si-1 Al^{IV}_s should not change appreciably, in agreement whith the experimental data. This is thus the favored hypothesis. However, other observations have to be accounted for, namely the disappearance, in CPB, of the Al^{IV}_p line and the shift of the Al^{IV}_s line toward a lower positive shift.

This is a clear indication that the pillar reorganization provoked by the thermal treatment is very different from that occurring in CPH and CPL. It explains the decrease in intensity of the Al^{IV} contribution to the ^{27}Al resonance line. In order to explain the shift, one may speculate that linking the pillar to the tetrahedral layer induces an inversion of an aluminum tetrahedron of the tetrahedral layer. This would lead to new Si–O–Al^{IV}_z linkage in which the negative charge of the aluminum tetrahedron is no longer buried in a continuous tetrahedral network but is exposed in the interlamellar space. The frequency shift of the Si-1 Al contribution should be in the same direction, as indeed observed.

Keeping the essential feature of the pillar, namely four layers of oxygen (or OH or H_2O) superimposed, the model shown in Figure 8 is one among a few that can be proposed, assuming that 13 Al atoms remain in the pillar. Also this model accounts for the fact that an appreciable dehydroxylation of the pillar must occur, whereas its positive charges must balance approximately the nearby negative charges of the inverted aluminum tetrahedra, Al^{IV}_z.

Statistically the bonding with the clay tetrahedral layers would involve three inverted tetrahedra per pillar. Those bonds may be responsible for a more perfect symmetry of the pillar aluminum octahedra and thus for the good agreement between the (Al^{VI}_p + Al^{VI}_s) contribution to the overall ^{27}Al signal (85.5%) and that calculated from the chemical analysis (84%). Thus the structural rearrangement in the pillar would contribute to suppress octahedral distortion.

In the suggested model of Figure 8, the two first oxygen (or OH or H_2O) layers in the pillar form six aluminum octahedra sharing edges, the aluminum atoms forming a hexagonal ring as in Figure 1. The second and third oxygen layers form four adjacent Al^{VI}_p octahedra separated by three octahedral vacancies. Three of these octahedra share faces with the bottom octahedral layer and edges with the fourth one. The top octahedral layer is formed from three Al^{VI}_p octahedra sharing edges. They share also edges with the second octahedral layer.

The pillar depicted in this way has the composition $[Al^{VI}_{13}(OH)_{12}(H_2O)_{15}]^{+}$. Three of the oxygen atoms would be shared with the inverted tetrahedra of the clay tetrahedral layers. The pillar should have a C_{3v} symmetry with a threefold symmetry axis and three planes of symmetry.

The transformation of the pillar shown in Figure 1 to that shown in Figure 8 involves mainly the loss of about 50% of the initial OH content, the rotation of the aluminum octahedra in the second octahedral layer, and the loss of Al^{IV}_p.

Thus, pillaring beidellite with Al_{13} would result in seeding the growth of a tridimensional network grafted on the bidimensional network of the clay. Then the resulting high-area solid could be considered as a bidimensional zeolite.

The idea of inverting a tetrahedron of the tetrahedral layer resucitates to some extent a structure proposed by Edelman and Favejee,[34] who suggested that every alternate tetrahedron of the tetrahedral layers in smectites is inverted so that the apex points away from the surface instead of into the interior. In order to maintain the continuity of structure and the balance of charges, the apical O ion is changed into OH and another OH is placed in the hole that is left in the octahedral layer. It was shown (Brown[35]) that this structure is incompatible with X-ray diffraction data observed for smectites and with the origin of the cation-exchange capacity. These arguments, however, do not exclude the possible inversion of some tetrahedra and especially those where Si by Al isomorphic substitution creates structural misfits when a chemical driving force is applied.

The specific surface area obtained by the BET method (N_2 at −196 °C) for CPB is 315 m^2/g ± 2% (five samples) after drying at 220 °C, whereas the micropore volume determined by the Dubinin equation[34] is 0.17 cm^3 ± 10%. Assuming a regular hexagonal distribution of the pillars and an area of 110 $Å^2$ per pillar, the interlamellar porosity should be 0.18 cm^3/g for a spacing of 17.5 Å and clay sheet thickness of 10 Å.

The average (six samples) surface area and micropore volume for a pillared and calcined Wyoming bentonite with structural formula $Na_{0.06}1.65Al^{(13)}Si^{IV}_8(Al_3Mg_{0.65}Fe_{0.35})^{VI}O_{24.2}$ are 251 m^2/g (±8%) and 0.115 cm^3/g (±10%) after drying at 220 °C, respectively (Plee and Fripiat[24]).

The main textural difference between CPB and calcined pillared montmorillonite is thus in the micropore volume.

Discussion

Pillaring and calcining pillared smectites with or without Al substitutions in tetrahedral layers have some striking resemblances but also some striking differences. The main resemblance is that pillaring at 18 Å results obviously from the selective adsorption of an aluminum hydroxy polymer whose ^{27}Al NMR spectroscopic features are identical with those of the Al_{13} species in solution. The main difference is that in smectite without tetrahedral substitution the tetrahedral layer does not react with the pillars.

The principal difficulty met in this work is connected with the quantitative interpretation of the results of the high-resolution solid-state ^{27}Al MAS-NMR spectra. In aluminosilicates according to Ghose et al.[30] the quadrupole coupling constant for AlO_4 tetrahedra depends mostly on shear strain (ψ)

$$|\psi| = \sum_i |\tan(\theta_i - \theta_0)| \qquad (3)$$

where θ_i is the individual O–Al–O bond angle and $\theta_0 = 109.5°$ (the ideal bond angle), whereas for AlO_6 octahedra, the quadrupole coupling is mostly a function of the longitudinal strain (α)

$$|\alpha| = \sum |\ln l_i/l_0| \qquad (4)$$

(34) Edelman, C. H.; Favejee, J. C. L. *Z. Kristallogr. Kristallgeom., Kristallphys., Kristallchem.* **1940**, *102*, 417.

(35) Brown, G. "the X-Ray Identification and Crystal Structure of Clay Minerals"; Mineralogical Society: London, 1961; p 152.

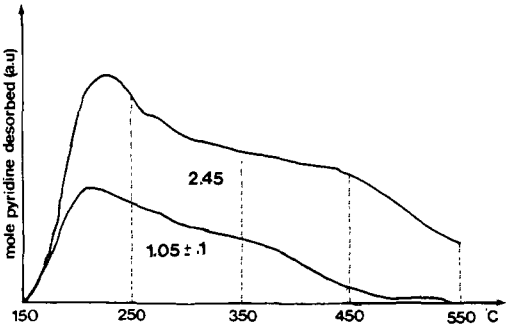

Figure 9. Thermodesorption of pyridine: top, CPB; bottom; CPM. The total numbers of desorbed pyridine molecules are shown in enclosures (mmol/g).

where l_i is the individual Al–O bond length and l_0 the "ideal" bond length. Intercalation and thermal transformation must change the quadrupole coupling constant of $Al^{VI}{}_p$.

When the distribution of the aluminum species among the various sites obtained from the integration of the ^{27}Al spectra reported in Table V is compared either with the chemical structural formulas of B and PB or with the theoretical composition of the Al_{13} polymer, it is clear that the larger the fwhh, the larger the discrepancies.

The effect of a broad fwhh combined with an asymmetric sideband pattern leads obviously to large disagreements as those reported for CPH, PL, and CPL.

On the contrary, when, like in beidellite, the $Al^{IV}{}_s$ and $Al^{VI}{}_s$ signals have fwhh below or of the order of 10 ppm, the agreement is acceptable.

Of course, in aluminum-bearing beidellite, the pillar aluminum content contributes much less to the overall aluminum content than in the pillared hectorite or laponite where the clays do not contain aluminum. Therefore even if the good quantitative agreement between the NMR and chemical Al^{IV} content in CPB should support a structural arrangement such as that proposed in Figure 8, the only safe conclusion is that in the thermally modified pillar, in CPB, the pillar octahedra achieve a higher symmetry than in the two other smectites.

It is evident that the structure proposed for the bidimensional zeolite CPB that would contain the Si–O–$Al^{IV}{}_z$ linkage characteristic of a Y zeolite is hypothetical and that it has to be supported by experimental facts.

Those already suggested are that inverting aluminum tetrahedra in the tetrahedral layer and anchoring their apex oxygen pointing out into the interlamellar space to the pillar would reduce adequately the overall lattice negative charge and could explain the formation of the $Al^{IV}{}_z$ sites at δ 56.5 (instead of δ 67.5 for $Al^{IV}{}_s$) and the shift of the ^{29}Si signal of the Si–O–$Al^{IV}{}_z$–O$Al^{VI}{}_p$ contribution from −90.5 to −92.5.

In clays without tetrahedral Al substitution, besides the van der Waals contribution, the positively charged pillars have to balance the clay negative charge. There is no reason for this electrostatic contribution to increase the symmetry in the pillar structure, and in fact, it has been shown that calcining pillared clays increases the overall contribution of $Al^{VI}{}_p$ to the ^{27}Al signal. However, the uncertainty in the relative $Al^{IV}{}_p$ and $Al^{IV}{}_p$ contents in CPH and CPL does not allow one to suggest a structure for the dehydroxylated pillars in these clays. On the contrary, when a chemical link between the pillar and the sheet exists as in CPB, the octahedral distortion in the pillar is much reduced.

From a chemical point of view, in CPB the Si–O–$Al^{IV}{}_z$ linkages should induce a larger number of stronger acid sites as compared to those in CPM. This is indeed the fact. Figure 9 shows the temperature-programmed desorption (4 °C/min) of pyridine preadsorbed at 150 °C by CPB and by a calcined pillared montmorillonite (CPM). Sampling the desorbed species was carried out every minute.

Obviously the difference in the acid properties of CPB and CPM is such that it could not be explained without assuming the presence in CPB of acid sites bearing a strong resemblance to those existing in acid Y zeolites, as shown recently.[25] Moreover, it will be shown elsewhere that the catalytic properties of CPB for cracking and hydroisomerization of *n*-hexane and *n*-decane are very comparable with those of Y zeolites and very different from those of CPM.

Finally we conclude that (i) pillaring beidellite and smectites to 18 Å with aluminum hydroxy polymers results from the intercalation of the Al_{13} species by a cation-exchange process, (ii) calcining pillared smectites without tetrahedral substitution does not modify the clay tetrahedral layer and does not transform the pillar into a pseudospinel, whereas (iii) calcining pillared beidellite results in the formation of linkages between the clay sheets and the Al_{13} pillars. These linkages could be achieved by inverting aluminum tetrahedra of the clay tetrahedral layer, leading therefore to a local environment that can be considered as characteristic of a bidimensional zeolite. This hypothesis deserves further studies.

Acknowledgments. This work would not have been possible without the help of Professors E. Oldfield and Jonas of the University of Illinois at Urbana-Champaign and the technical assistance of B. Montez. Discussions with A. Schutz and G. Poncelet of the University of Louvain were very fruitful. D.P. is indebted to the Compagnie Française de Raffinage for financial support during his Ph.D. thesis.